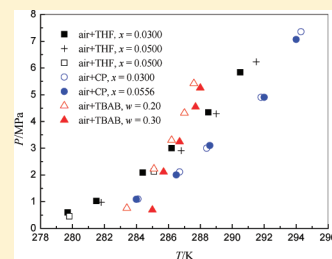


# Hydrate Dissociation Conditions for Mixtures of Air + Tetrahydrofuran, Air + Cyclopentane, and Air + Tetra-*n*-butyl Ammonium Bromide

Hongjun Yang, Shuanshi Fan, Xuemei Lang, Yanhong Wang,\* and Xulin Sun

Key Laboratory of Enhanced Heat Transfer and Energy Conservation, Ministry of Education, School of Chemistry and Chemical Engineering, South China University of Technology, Guangzhou 510640, China

**ABSTRACT:** Substantial oxygen enrichment is observed in the natural air hydrates formed in Arctic and Antarctic ice sheets. Inspired by this phenomenon, a novel air separation method, utilizing hydrate crystallization, is proposed in our work. The three-phase equilibrium pressure for the air + water system is greater than 15 MPa as the temperature is upon ice point, which makes the air separation impractical by hydrate formation under mild temperature conditions. So, some additives were selected to reduce the phase equilibrium pressure of air hydrates at a fixed temperature. In this work, hydrate dissociation conditions for the air + tetrahydrofuran (THF) + water system ( $x = 0.0300$  and  $0.0500$ ), the air + cyclopentane (CP) + water system ( $x = 0.0300$  and  $0.0556$ ), and the air + tetra-*n*-butyl ammonium bromide (TBAB) + water system ( $w = 0.20$  and  $0.30$ ) were measured in the temperature ranges of (279.7 to 290.5) K, (284.0 to 296.2) K, and (283.4 to 288.0) K, respectively. The comparison result shows that, in the pressure range of (0 to 1.5) MPa, the promotion effect of these three additives on the air + water system follows TBAB > CP > THF.



## INTRODUCTION

Clathrate hydrates or gas hydrates are crystalline ice-like compounds, in which small molecules such as methane, nitrogen, and oxygen, and so forth are trapped in the cages composed of hydrogen-bonded water molecules.<sup>1</sup> Air hydrates are found in Arctic and Antarctic ice sheets, where during snowfalls, air was trapped inside to form stable hydrates under high-depth and low-temperature conditions. Air hydrates in ice cores were first reported by Shoji et al.<sup>2</sup> and usually form an sII crystal structure.<sup>3</sup> A fractionation effect of air hydrates for an oxygen mole fraction of roughly 0.37 was observed in air hydrates.<sup>4–6</sup> Therefore, oxygen in the air can be enriched by the formation of air hydrates.

Phase equilibrium information of air hydrates is essential and vital to air separation using hydrate formation. There are reports on the hydrate phase equilibrium data for the air + water system in the ice–hydrate–vapor (I–H–V) region<sup>5,7</sup> and in the liquid water–hydrate–vapor (Lw–H–V) region.<sup>8</sup> The three-phase (Lw–H–V) equilibrium pressure for the air + water system is greater than 15 MPa when the temperature is above the ice point,<sup>7</sup> which renders it impractical to perform air separation using hydrate formation. Hence, reducing hydrate phase equilibrium pressure under mild temperature conditions is a key step toward air separation based on hydrate crystallization.

Adding a compound, such as 1,4-epoxybutane, also known as tetrahydrofuran (THF), to a single gas + water system is a feasible method to reduce the hydrate phase equilibrium pressure at a fixed temperature.<sup>9–11</sup> In our previous work,<sup>9</sup> four-phase Lw–A (additive)–H–V equilibrium data for the air + THF + water system were measured in the temperature range of (281.84 to 299.41) K, and the results show that the hydrate

phase equilibrium pressure for the air + water system can be reduced to 0.918 MPa at 281.84 K by the addition of THF at  $x = 0.0500$  ( $x$  and  $w$  represent the mole fraction and mass fraction of additive in the aqueous solution, respectively), which indicates it is feasible for air separation based on hydrate crystallization under mild temperature and pressure conditions by the addition of a promoter.

Cyclopentane (CP) can form single sII hydrate with water at the temperature around 280 K at atmospheric pressure.<sup>1,12</sup> Similar to THF, CP molecules reside only in the large cages, and the small ones are left to be vacant.<sup>1,13</sup> Single gas molecules can occupy the vacant small cages in the CP hydrate under low pressure and high temperature conditions.<sup>1</sup> In addition, *N,N,N*-tributyl-1-butylammonium bromide, also known as tetra-*n*-butylammonium bromide (TBAB), can form semiclathrates with water at atmospheric pressure. Unlike THF or CP clathrate hydrate, in TBAB semiclathrates, anions ( $\text{Br}^-$ ) form cage structures with water molecules, and the tetra-*n*-butylammonium cations ( $\text{TBA}^+$ ) occupy four partially broken cages.<sup>14</sup> There are empty cages in TBAB semiclathrates which can capture small-sized gas molecules under mild pressure conditions.<sup>15</sup> Thus, it is possible that the hydrate phase equilibrium pressure for the air + water system would be decreased by the addition of CP or TBAB.

In this work, hydrate phase equilibrium data for the air + THF + water system ( $x = 0.0300$  and  $0.0500$ ), the air + CP + water system ( $x = 0.0300$  and  $0.0556$ ), and the air + TBAB + water system ( $w = 0.20$  and  $0.30$ ) were measured. The effect of

Received: December 14, 2011

Accepted: March 8, 2012

Published: March 19, 2012

additive concentration on hydrate dissociation conditions is investigated, and the promotion effects of the three additives are compared.

## EXPERIMENTAL SECTION

**Materials.** The materials used in this work, along with their purities and suppliers, are listed in Table 1. Deionized water

**Table 1. Materials Used in the Experiments**

component	purity	supplier
oxygen	$x \geq 0.99999$	Foshan Analytical Instrument Co., Ltd.
air (oxygen, $x_1 = 0.21$ ; nitrogen, $x_2 = 0.79$ )		Guangzhou Yuegang Gas Industry Co., Ltd.
tetrahydrofuran	$w \geq 0.99$	Sinopharm Chemical Reagent Co., Ltd.
cyclopentane	$w \geq 0.99$	Chengdu Kelong Chemical Company
tetra- <i>n</i> -butyl ammonium bromide	$w \geq 0.99$	Tianjin Kermel Chemical Reagent Co., Ltd.
water		deionized

was used in all experiments. THF, CP, TBAB, and water were weighted on an electronic balance with an accuracy of  $\pm 0.1$  mg.

**Experimental Apparatus.** The schematic diagram of the apparatus used to determine the hydrate phase equilibrium data for the mixtures is shown in Figure 1, which has also been

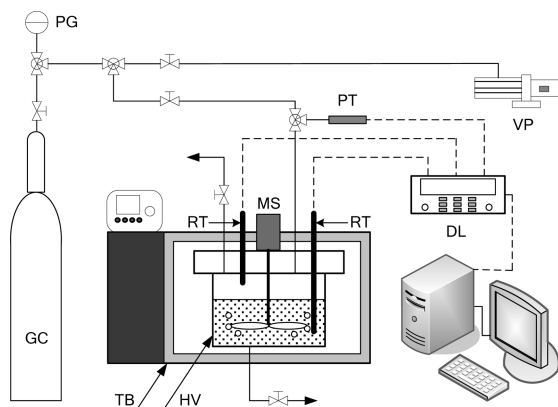


**Figure 1.** Schematic diagram of the experimental apparatus. DL, data logger; GC, gas cylinder; HV, hydrate vessel; MS, magnetic stirrer; PG, pressure gauge; PT, pressure transducer; RT, resistance thermometer; TB, thermostatic bath; VP, vacuum pump.

described by Li et al.<sup>16</sup> in our previous works. The main part of the apparatus is a stainless steel cylinder with an effective volume of about 300 cm<sup>3</sup> (Hai'an Oil Scientific Research Apparatus Company, China) and is equipped with a magnetic stirrer to agitate the content inside the vessel. The allowable operational pressure and temperature ranges for the vessel are (0 to 20) MPa and (252.15 to 423.15) K, respectively. The vessel is entirely immersed in a thermostatted bath (Huber CC2-K20B) for accurately controlling the vessel temperature. Two platinum resistance thermometers (Westzh WZ-PT100) with an uncertainty of  $\pm 0.1$  K are placed inside the vessel to measure the temperatures in the vapor and liquid phases. A pressure transducer (Senex DG-1300) with an accuracy of  $\pm 0.01$  MPa is used to measure the internal pressure of the vessel.

All of the data are recorded by a data logger (Agilent 34970A) in the time interval of 20 s.

**Experimental Method.** The hydrate dissociation conditions were measured using the reliable isochoric pressure-search method.<sup>17</sup> The vessel was well-cleaned with deionized water and the experimental aqueous solution successively, then was purged with the experimental gas for at least three times. Approximately 200 cm<sup>3</sup> of the aqueous solution was introduced into the vessel after being vacuumed. Gas was supplied from a gas cylinder into the vessel to a desired pressure level through a pressure-regulating valve. The valve was closed after the temperature and the pressure were stabilized in the vessel. Subsequently, the magnetic stirrer was initiated, and the temperature was decreased gradually at the cooling rate of 3 K·h<sup>-1</sup> to form hydrate. The hydrate formation in the vessel was detected by a decrease in  $P$  and an increase in  $T$ . The temperature was then increased in steps of 0.1 K, and (4 to 6) h was required to achieve adequate equilibrium state inside the vessel at each temperature step. For each experiment run, a heating  $P$ - $T$  curve could be obtained, the point at which the slope of the  $P$ - $T$  curve sharply changes was considered to be the hydrate dissociation point, where all hydrate crystals have dissociated completely.

## RESULTS AND DISCUSSION

To check the reliability of the experimental apparatus and the isochoric pressure-search method used in this work, hydrate dissociation conditions for the oxygen + CP + water system at  $x = 0.0556$  were measured and compared with the data in the literature. The experimental data are reported in Table 2 and

**Table 2. Hydrate Dissociation Conditions for the Oxygen + CP + Water System Measured at  $x = 0.0556$**

$T/K$	$P/\text{MPa}$
286.0	1.03
291.3	3.30
293.8	5.19
297.1	9.10

plotted in Figure 2, along with the data reported by Du et al.<sup>18</sup> Figure 2 shows a good agreement between the data we measured and those reported in the literature.

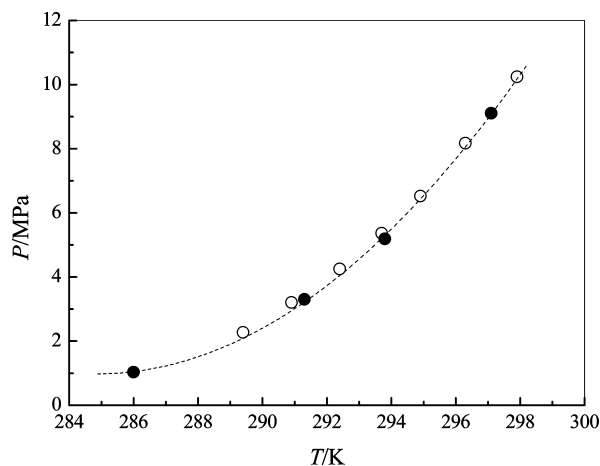


**Figure 2.** Hydrate phase equilibrium data for the oxygen + CP + water system:  $\circ$ ,  $x = 0.0556$ , Du et al.;<sup>18</sup>  $\bullet$ ,  $x = 0.0556$ , this work.

Four-phase (Lw–A–H–V) equilibrium data for the air + THF + water system, the air + CP + water system, and the air + TBAB + water system are reported in Tables 3, 4, and 5 and are

**Table 3. Hydrate Dissociation Conditions for the Air + THF + Water System Measured at  $x = 0.0300$  and  $0.0500$**

$T/K$	$P/MPa$
$x = 0.0300$	
279.7	0.60
281.5	1.03
284.4	2.09
286.2	3.00
288.5	4.34
290.5	5.84
$x = 0.0500$	
279.8	0.46
285.1	2.13

**Table 4. Hydrate Dissociation Conditions for the Air + CP + Water System Measured at  $x = 0.0300$  and  $0.0556$**

$T/K$	$P/MPa$
$x = 0.0300$	
284.0	1.09
286.5	2.00
288.6	3.10
292.0	4.90
294.0	7.06
$x = 0.0556$	
284.1	1.10
286.7	2.11
288.4	3.00
291.8	4.90
294.3	7.35
296.2	9.45

**Table 5. Hydrate Dissociation Conditions for the Air + TBAB + Water System Measured at  $w = 0.20$  and  $0.30$**

$T/K$	$P/MPa$
$w = 0.20$	
283.4	0.76
285.1	2.23
286.2	3.30
287.0	4.31
287.6	5.42
$w = 0.30$	
285.0	0.69
285.7	2.11
286.7	3.24
287.7	4.54
288.0	5.25

plotted in Figures 3, 4, and 5, respectively. In these figures, three-phase (I–H–V)<sup>7</sup> and (Lw–H–V)<sup>8</sup> hydrate dissociation conditions for the air + water system are also displayed to investigate the promotion effects of the additives used in this work. The hydrate promotion effect means that the hydrate stability zone for the air + water system is shifted to the low pressure or high temperature zone due to the presence of additive.<sup>13</sup> From Figure 3 it can be seen that hydrate phase equilibrium pressure for the air + water system is reduced by at least 30 MPa at a given temperature in the temperature range of

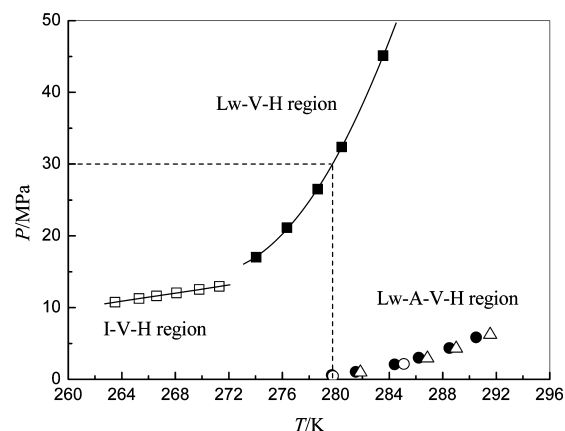


**Figure 3.** Hydrate phase equilibrium data for the air + water system and the air + THF + water system. Air + water system:  $\square$ , Mohammadi and Richon;<sup>7</sup>  $\blacksquare$ , Mohammadi et al.;<sup>8</sup> air + THF + water system:  $\bullet$ ,  $x = 0.0300$ , this work;  $\circ$ ,  $x = 0.0500$ , this work;  $\triangle$ ,  $x = 0.0500$ , Yang et al.;<sup>9</sup> —, best fit.

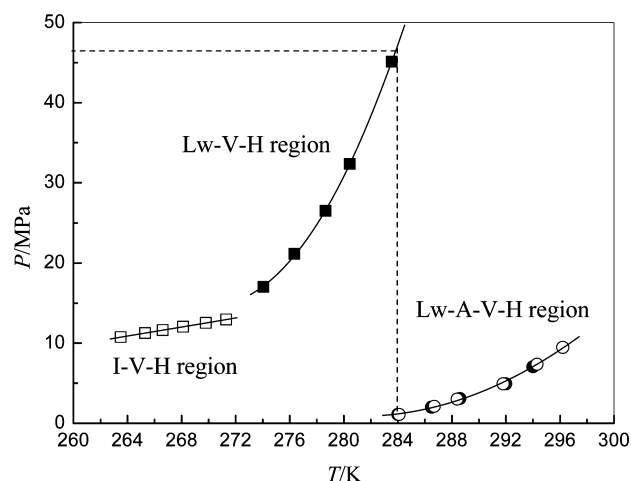


**Figure 4.** Hydrate phase equilibrium data for the air + water system and the air + CP + water system. Air + water system:  $\square$ , Mohammadi and Richon;<sup>7</sup>  $\blacksquare$ , Mohammadi et al.;<sup>8</sup> air + CP + water system:  $\bullet$ ,  $x = 0.0300$ , this work;  $\circ$ ,  $x = 0.0556$ , this work; —, best fit.

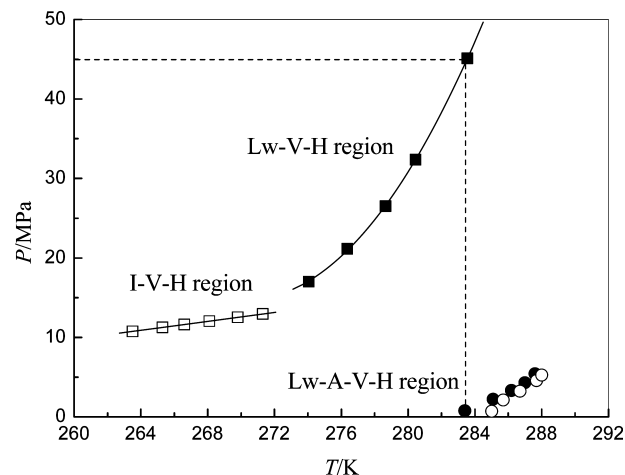


**Figure 5.** Hydrate phase equilibrium data for the air + water system and the air + TBAB + water system. Air + water system:  $\square$ , Mohammadi and Richon;<sup>7</sup>  $\blacksquare$ , Mohammadi et al.;<sup>8</sup> air + TBAB + water system:  $\bullet$ ,  $w = 0.20$ , this work;  $\circ$ ,  $w = 0.30$ , this work; —, best fit.

(279.7 to 290.5) K by introducing THF ( $x = 0.0300$  and  $0.0500$ ). The higher concentration of THF leads to the lower equilibrium pressure at a specific temperature. Figure 4 shows that, at the same temperature in the temperature range of (284.0 to 296.2) K, the four-phase (Lw–A–H–V) equilibrium pressure for the air + CP + water system ( $x = 0.0300$  and  $0.0556$ ) is lower by at least 45 MPa than the three-phase (Lw–H–V) equilibrium pressure for the air + water system. However, the change in the concentration of CP has little influence on the hydrate dissociation conditions for the air + CP + water system, which may be due to that CP is insoluble in water, and the change in the amount of CP in water does not affect the chemical potential of water.<sup>19</sup> The promoter effect of TBAB on hydrate formation is also observed in the air + water system. As shown in Figure 5, the hydrate phase equilibrium pressure for the air + water system is reduced by at least 45 MPa at a specific temperature in the temperature range of (283.4 to 288.0) K due to the presence of TBAB measured at  $w = 0.20$  and  $0.30$ , respectively. At a fixed temperature, the hydrate dissociation pressure decreases with the increase in the concentration of TBAB. The comparison of hydrate equilibrium data for the air + water system in the presence of THF, CP, or TBAB is illustrated in Figure 6. The slope of  $P$ – $T$  curve

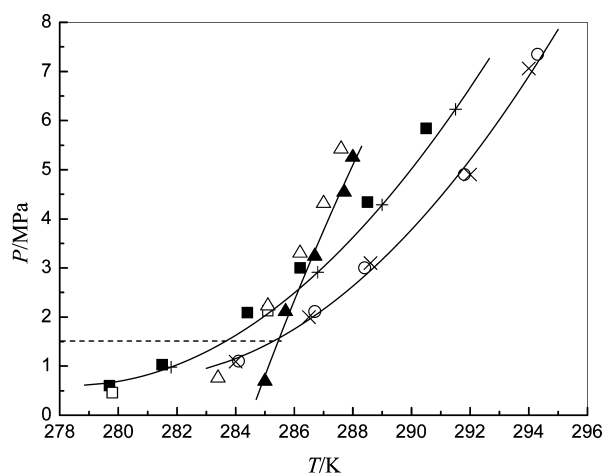


**Figure 6.** Comparison of hydrate phase equilibrium data for the air + THF + water system, the air + CP + water system, and the air + TBAB + water system. Air + THF + water system: ■,  $x = 0.0300$ , this work; □,  $x = 0.0500$ , this work; +,  $x = 0.0500$ , Yang et al.;<sup>9</sup> air + CP + water system: ○,  $x = 0.0300$ , this work; ×,  $x = 0.0556$ , this work; air + TBAB + water system: △,  $w = 0.20$ , this work; ▲,  $w = 0.30$ , this work; —, best fit.

of the air + TBAB + water system is greater than those of the air + THF + water and the air + CP + water systems, which indicates that the former system is more sensitive to temperature than the latter systems. The hydrate phase equilibrium temperature at a specific pressure in the pressure range of (0 to 1.5) MPa follows TBAB + air + water system ( $w = 0.30$ ) > air + CP + water system ( $x = 0.0556$ ) > air + THF + water system ( $x = 0.0500$ ).

## CONCLUSIONS

This work reports the hydrate dissociation conditions for the air + THF + water system ( $x = 0.0300$  and  $0.0500$ ), the air + CP + water system ( $x = 0.0300$  and  $0.0556$ ), and the air + TBAB + water system ( $w = 0.20$  and  $0.30$ ) in the temperature ranges of (279.7 to 290.5) K, (284.0 to 296.2) K, and (283.4 to

288.0) K, respectively. The isochoric pressure-search method is used to determine all hydrate dissociation conditions. Good agreement between the hydrate dissociation data obtained in this work for the oxygen + CP + water system ( $x = 0.0556$ ) and those reported by Du et al.<sup>18</sup> confirms the reliability of the experimental apparatus and the method employed in this work. The results show that three-phase (Lw–H–V) equilibrium pressure for the air + water system can be significantly reduced by introducing THF, CP, or TBAB. At a fixed pressure in the pressure range of (0 to 1.5) MPa, the four-phase (Lw–A–H–V) equilibrium temperature for the air + TBAB + water system ( $w = 0.30$ ) is higher than those for the air + CP + water system ( $x = 0.0556$ ) and the air + THF + water system ( $x = 0.0500$ ). Therefore, among the three additives, TBAB may be the strongest promoter to be applied to air separation using hydrate formation in the working pressure range of (0 to 1.5) MPa.

## AUTHOR INFORMATION

### Corresponding Author

\*Tel.: + 86-20-22236581. Fax: +86-20-22236581. E-mail: wyh@scut.edu.cn.

### Funding

The work was supported by the National Natural Science Foundation of China (Grant No. 51176051), the National Basic Research Program of China ("973" Program) (Grant No. 2009CB219504-03), and the Colleges and Universities High-level Talents Program of Guangdong.

### Notes

The authors declare no competing financial interest.

## REFERENCES

- (1) Sloan, E. D.; Koh, A. H. *Clathrate Hydrates of Natural Gases*, 3rd ed.; CRC Press/Taylor & Francis: Boca Raton, FL, 2008.
- (2) Shoji, H.; Langway, C. C. Jr. Air Hydrate Inclusions in Fresh Ice Core. *Nature* **1982**, *298*, 548–550.
- (3) Hondoh, T.; Anzai, H.; Goto, A.; Mae, S.; Higashi, A.; Langway, C. C. Jr. The Crystallographic Structure of the Natural Air-Hydrate in Greenland Dye-3 Deep Ice Core. *J. Inclusion Phenom. Macroscopic Chem.* **1990**, *8*, 17–24.
- (4) Nakahara, J.; Shigesato, Y.; Higashi, A.; Hondoh, T.; Langway, C. C. Jr. Raman Spectra of Natural Clathrates in Deep Ice Cores. *Philos. Mag. B* **1998**, *57*, 421–430.
- (5) Kuhs, W. F.; Klapproth, A.; Chazallon, B. Chemical Physics of Air Clathrate Hydrates. In *Physics of Ice Core Records*; Hondoh, T., Ed.; Hokkaido University Press: Sapporo, 2000; pp 373–393.
- (6) van der Waals, J. H.; Platteeuw, J. C. Clathrate Solutions. *Adv. Chem. Phys.* **1959**, *2*, 1–57.
- (7) Mohammadi, A. H.; Richon, D. Ice–Clathrate Hydrate–Gas Phase Equilibria for Air, Oxygen, Nitrogen, Carbon Monoxide, Methane, or Ethane + Water System. *Ind. Eng. Chem. Res.* **2010**, *49*, 3976–3979.
- (8) Mohammadi, A. H.; Tohidi, B.; Burgass, R. W. Equilibrium Data and Thermodynamic Modeling of Nitrogen, Oxygen, and Air Clathrate Hydrates. *J. Chem. Eng. Data* **2003**, *48*, 612–616.
- (9) Yang, H. J.; Fan, S. S.; Lang, X. M.; Wang, Y. H. Phase Equilibria of Mixed Gas Hydrates of Oxygen + Tetrahydrofuran, Nitrogen + Tetrahydrofuran, and Air + Tetrahydrofuran. *J. Chem. Eng. Data* **2011**, *56*, 4152–4156.
- (10) Anderson, R.; Chapoy, A.; Tohidi, B. Phase Relations and Binary Clathrate Hydrate Formation in the System  $H_2$ -THF- $H_2O$ . *Langmuir* **2007**, *23*, 3440–3444.
- (11) Mohammadi, A. H.; Martinez-Lopez, J. F.; Richon, D. Determining Phase Diagrams of Tetrahydrofuran plus Methane, Carbon Dioxide or Nitrogen Clathrate Hydrates Using an Artificial Neural Network Algorithm. *Chem. Eng. Sci.* **2010**, *65*, 6059–6063.

- (12) Fan, S. S.; Liang, D. Q.; Guo, K. H. Hydrate Equilibrium Conditions for Cyclopentane and a Quaternary Cyclopentane-Rich Mixture. *J. Chem. Eng. Data* **2001**, *46*, 930–932.
- (13) Mohammadi, A. H.; Richon, D. Phase Equilibria of Clathrate Hydrates of Cyclopentane + Hydrogen Sulfide and Cyclopentane + Methane. *Ind. Eng. Chem. Res.* **2009**, *48*, 9045–9048.
- (14) Dyadin, Y. A.; Bondaryuk, I. V.; Aladko, L. S. Stoichiometry of Clathrates. *J. Struct. Chem.* **1995**, *36*, 995–1045.
- (15) Lee, S.; Park, S.; Lee, Y.; Lee, J.; Lee, H.; Seo, Y. Guest Gas Enclathration in Semiclathrates of Tetra-*n*-butylammonium Bromide: Stability Condition and Spectroscopic Analysis. *Langmuir* **2011**, *27*, 10597–10603.
- (16) Li, S. F.; Fan, S. S.; Wang, J. Q.; Lang, X. M.; Wang, Y. H. Semiclathrate Hydrate Phase Equilibria for CO<sub>2</sub> in the Presence of Tetra-*n*-butyl Ammonium Halide (Bromide, Chloride, or Fluoride). *J. Chem. Eng. Data* **2010**, *55*, 3212–3215.
- (17) Tohidi, B.; Burgass, R. W.; Danesh, A.; Østergaard, K. K.; Todd, A. C. Improving the Accuracy of Gas Hydrate Dissociation Point Measurements. *Ann. N.Y. Acad. Sci.* **2000**, *912*, 924–931.
- (18) Du, J. W.; Liang, D. Q.; Li, D. L.; Li, X. J. Experimental Determination of the Equilibrium Conditions of Binary Gas Hydrates of Cyclopentane plus Oxygen, Cyclopentane plus Nitrogen, and Cyclopentane plus Hydrogen. *Ind. Eng. Chem. Res.* **2010**, *49*, 11797–11800.
- (19) Zhang, L. W.; Huang, Q.; Sun, C. Y.; Ma, Q. L.; Chen, G. J. Hydrate Formation Conditions of Methane + Ethylene + Tetrahydrofuran + Water Systems. *J. Chem. Eng. Data* **2006**, *51*, 419–422.